

Optical Properties of Dissolved Organic Matter in Finnish and Estonian Lakes

L. Sipelgas¹, H. Arst¹, K. Kallio², A. Erm¹,
P. Oja³ and T. Soomere¹

¹TTU Marine Systems Institute

²Finnish Environmental Institute

³University of Tartu

The main objective of the present study is to test various methods for describing the absorption spectra of coloured dissolved organic matter (CDOM) and to determine the numerical values of some optical parameters of CDOM in lakes with diverse water quality. First, the parameters of an exponential model in different spectral intervals were determined. In addition, the suitability of some other models for the approximation of CDOM spectra was estimated. Specific absorption coefficients of CDOM were calculated from the absorption coefficients and dissolved organic carbon (DOC) concentrations. The experimental initial data were differences between spectral attenuation coefficients of filtered and distilled water. Two datasets were used: 1) for 13 Estonian and 7 Finnish lakes (altogether 404 spectra between 350 and 700 nm) measured by the Estonian Marine Institute (EMI); 2) for 10 Finnish lakes (73 spectra) measured by the Finnish Environment Institute (FEI).

The spectra of CDOM absorption coefficients (a_{CDOM}) were calculated from experimental data taking into account the correction due to scattering properties of colloids in the filtered water. The total content of CDOM in natural waters of Estonian and Finnish lakes was expressed by means of a_{CDOM} at the wavelength of 380 nm. It varied significantly, from 0.71 to 19.5 m⁻¹, the mean value (of all the investigated lakes) being around 6.6 m⁻¹. Slopes of the exponential approximation varied widely, from 0.006 to 0.03 nm⁻¹. Averaged over all lakes values of slope for the interval 380-500 nm obtained from the EMI dataset are close to those obtained from the FEI dataset: from 0.014 nm⁻¹ (without correction) to 0.016-0.017 nm⁻¹ (with different types of correction). These results are in good correspondence with most published data.

Attempts to describe the spectra in the region of 350-700 nm by means of hyperexponential functions ($\sim \exp(-\alpha\lambda^\eta)$) show that: (1) $\eta < 1$ (in the case of

traditional exponential approximation $\eta = 1$); (2) a promising idea is to seek the best fit only for wavelengths $\lambda > \lambda_1$, where λ_1 will be chosen taking into account the real shape of a_{CDOM} spectra.

The mean value of the specific absorption coefficient (a^*_{CDOM}) at the wavelength 380 nm obtained in this study ($0.44 \text{ L mg}^{-1} \text{ m}^{-1}$) is close to the values published in the literature, if we assume that $a^*_{CDOM}(380)$ is calculated using the data of dissolved organic matter (DOM). The optically non-active fraction of DOM in our study was high and therefore $a^*_{CDOM}(380)$ was considerably higher ($1.01 \text{ L mg}^{-1} \text{ m}^{-1}$) than $a^*_{CDOM}(380)$.

The results of the present work could be used in the modeling of underwater light field as well as in the interpretation of radiation measurements and optical remote sensing results.

Introduction

As known, dissolved organic matter (DOM) in natural water bodies is not identifiable as a distinct molecule, but it is a rather indeterminate mixture of dissolved organic substances (Dera 1992). Its chromophore-containing compounds contribute significantly to the total light absorption in the water. These optically active substances are mostly referred to as coloured dissolved organic matter (Hoge *et al.* 1993; Kallio 1999) or chromophoric dissolved organic matter, CDOM (Miller *et al.* 2000). Dissolved organic matter is an important variable of the water ecosystem and has an impact on the water colour and quality (Kalle 1938, 1966; Kirk 1976, 1983; Kopelevich 1983; Dera 1992). Together with phytoplankton and other aquatic plants CDOM (through absorption of light particularly at the blue end of the spectrum) competes for the capture of available light energy in water (Davies-Colley and Vant 1987; Kirk 1976, 1980). The absorption properties of CDOM have an important role also in the estimation of photochemical mineralization of dissolved organic carbon (Vähätalo *et al.* 2000). In remote sensing, the estimation of phytoplankton or suspended matter concentrations can be disturbed by the optical influence of CDOM, especially when they vary simultaneously (Davies-Colley and Vant 1987; Morel and Prieur 1977; Bukata *et al.* 1983).

The nature of CDOM is complicated to determine, but we do know that CDOM consists of complex organic compounds formed as a result of the metabolism and breakdown of organisms living in the aquatic environment or carried into it (Dera 1992). A large fraction of the CDOM, especially in lakes and coastal waters, may be derived from soil leaching and surface runoff (transported mainly by rivers). The remainder may be derived from degradation and breakdown of plankton and other aquatic organisms (Kalle 1966; Kirk 1983; Kopelevich 1983; Davies-Colley and Vant 1987). According to Kalle (1966), some of the more important and commonly found substances of CDOM are melanoids. Besides these, many other complex organic compounds have been found in the seawater, but their structures are for the moment somewhat hypothetical. Stuermer (1975) and Gagosian and Stuermer

(1977) reported that hydrocarbon fragments, amino acids, amino sugars, organic acids, and aromatic rings may be present. According to Højerslev (1980), Davies-Colley and Vant (1987) and Carder *et al.* (1989) the compounds of CDOM fall into two main groups: 1) phenolhumic (humic) acids, and 2) carbohydrate humic (fulvic) acids or melanoids. Note, that there exists also another definition for humic and fulvic acids (Aiken *et al.* 1988), which includes differences in size (it may be appropriate in the interpretation of optical spectra).

Besides dissolved matter CDOM may also contain some fine suspended particles. It is by no means simple to distinguish between these two phases because of the size of many of their molecules and their ability to flocculate, that is to come out of solution and form colloids (particles in the size range of 1-1000 nm), fine suspensions, or organic clusters (Dera 1992). Important is that the humic acid in fresh waters has been shown to be a colloid in the size range 70-250 nm (Ledin *et al.* 1993). Applicable analytical methods for determining CDOM in seawater have been developed, but it is extremely difficult to determine individual organic compounds therein (Dera 1992). Investigations of numerous researchers have shown that optical determination of CDOM has distinct advantages over chemical analytic techniques (Bricaud *et al.* 1981; Baker and Smith 1982; Kopelevich 1983; Davies-Colley and Vant 1987; Ferrari and Tassan 1991; Dera 1992). In using optical methods, CDOM is referred to in order to describe the optical properties of any dissolved organic matter, regardless of its origin and chemical composition (Bricaud *et al.* 1981). That convention, although questionable from a chemical point of view, enables us to include in a single parameter any dissolved matter causing variations in the water colour. Consequently, the influence of CDOM is expressed through the absorption coefficient of the filtered water at a given wavelength in UV or visible regions.

As known, filtered water may remain a scattering medium even after filtration because small particles pass through the filter. These scattering colloids may include fine inorganic particles as well as colloidal forms of aquatic humus, which appear to coexist with CDOM (Bricaud *et al.* 1981; Davies-Colley and Vant 1987). For such a medium the coefficient actually obtained by using a conventional spectrophotometer is intermediate between the beam attenuation coefficient and the absorption coefficient. The relationship between the true and apparent absorption is given by Bricaud *et al.* (1981)

$$a_{CDOM}(\lambda) = \chi(\lambda) - \beta(\lambda) \quad (1)$$

where $a_{CDOM}(\lambda)$ is the absorption coefficient of CDOM at the wavelength λ , $\chi(\lambda)$ is the spectrophotometrical measurement result and $\beta(\lambda)$ is the correction that takes into account the residual scattering in $\chi(\lambda)$. The algorithms used by different authors to describe $\beta(\lambda)$ are in general similar, but their numerical constants can differ markedly from each other (Bricaud *et al.* 1981; Davies-Colley 1983; Davies-Colley and Vant 1987; Blough *et al.* 1993; Green and Blough 1994; Gallie 1994; Kowalczyk and Kaczmarek 1996; Mäekivi and Arst 1996; Vodacek *et al.* 1997; Kowalczyk

1999; Aas 2000). Some authors do not apply any correction when investigating the absorption spectra of CDOM (*e.g.* Højerslev 1980; Carder *et al.* 1989; Nelson and Guarda 1995; Højerslev and Aas 1998). As known, the measured attenuation curve of CDOM in the red part of the spectrum is often unstable, which indicates essential relative errors of measurements. This brings about uncertainty in the calculation of correction.

Usually the absorption spectra of CDOM are described by an exponent (for the whole PAR region (350-700 nm) or some part of it). The values of the slope of this exponent have been presented by numerous authors, who recommend very different values as a reasonable mean. For oceanic water the slope varies from 0.004 to 0.053 (results by different authors cited by Aas 2000). Of course, its value depends on the composition of CDOM and size of colloids; however, practically no data describing this dependence in detail are available. Carder *et al.* (1989), analysing water samples taken from the Gulf of Mexico, determined the slope separately for fulvic acid and humic acid, obtaining respectively 0.0184 and 0.0110 nm⁻¹. Spatial distribution of the slope for CDOM off the coast of Georgia, U.S.A., calculated from SeaWiFS normalized water-leaving radiance data in January 1998 is shown in the paper by Miller *et al.* (2000). Their results indicated that the slope is steeper offshore and shallower inshore. However, data of this kind are very rare and additional investigations are needed.

In the underwater radiation and remote sensing studies not only the spectral absorption coefficient of CDOM throughout the visible range, but also its specific absorption coefficient a^*_{CDOM} (which is used to convert the absorption coefficient into the concentration of aquatic humus) is needed. However, only a few investigations have been made with both absorption coefficient and CDOM concentration measurements required for the determination of specific absorption coefficient (data given in Nyquist 1979; Jerlov 1968, Stuermer 1975; Højerslev 1980; Bricaud *et al.* 1981; Okami *et al.* 1982; Kallio 1999). The values of a^*_{CDOM} depend on the composition of CDOM and therefore we cannot expect to obtain one, universal spectrum. This is confirmed also by results published by authors mentioned above, where the value of a^*_{CDOM} varies from 0.275 to 2.16 L mg⁻¹ m⁻¹. To find out the variability and typical values of specific absorption coefficient for different water bodies and regions numerous and extensive investigations are needed.

The main objective of this study was to estimate the suitability and to determine the parameters of an exponential model for describing the absorption spectra of CDOM between 350 and 700 nm in lakes with diverse water quality. In addition, specific absorption coefficients of CDOM were calculated from the absorption coefficients and DOC concentrations. The results of the present work can be used in modelling of the total absorption coefficient spectra in lakes, which are needed for interpretation of underwater solar radiation data and for building the remote sensing models. Knowing optical properties of CDOM is important also for determining biogeochemical carbon fluxes.

Materials and Methods

Investigated Characteristics and Lakes

The spectrophotometers we used (described below) measure the difference between the attenuation coefficient of filtered (or natural) water and distilled water: $c^*_f(\lambda) = c_f(\lambda) - c_d(\lambda)$. Note that $c^*_f(\lambda)$ is identical to $\chi(\lambda)$ in Eq. (1), but it is not identical to a_{CDOM} , because some very small mineral particles can also pass through the filter.

We used two datasets of $c^*_f(\lambda)$ measured from filtered water:

- 1) $c^*_f(\lambda)$ for 13 Estonian and 7 Finnish lakes in the range of 350-700 nm (altogether 404 spectra, 36 recordings in each spectrum) measured by the Estonian Marine Institute (EMI) during the period 1994-99, and
- 2) $c^*_f(\lambda)$ for 10 Finnish lakes in the range 380-800 nm (73 spectra) measured by the Finnish Environment Institute (FEI) in 1997.

In addition, concentrations of DOC were determined from the FEI dataset. Because

Table 1– Lake type and area, minimum and maximum values of chlorophyll *a* concentration (C_{chl}) and Secchi disk depth (z_{SD}), the number of water samples used for determining the absorption spectra of CDOM (*n*) and years of measurements in the EMI dataset. “E” designates Estonian lake, “F” is Finnish lake.

Lake	Area, ha	Lake type	C_{chl} , $\mu\text{g L}^{-1}$	z_{SD} , m	<i>n</i>	Years
Päijänne (F)	7030	Oligotrophic	1.3-5.4	3.5-6.5	10	1995,1998-99
Paukjärv (E)	8.6	Oligotrophic	1.4-24.2	4.0-6.2	21	1997-99
Puujärvi (F)	700	Oligotrophic	3.6-6.1	3.0-6.0	2	1997
Nohipalu Valgjärv (E)	6.3	Oligotr./mesotr.	1.2-66	3.5-7.0	37	1994-99
Koorküla Valgjärv (E)	44.1	Oligotr./eutr.	1.8-15.0	2.9-5.3	20	1996-99
Kurtna Nõmmjärv (E)	15.6	Mesotrophic	0.7-33	2.5-4.5	13	1994-96
Linajärv (E)	5.8	Mesotrophic	9.3-87	1.25-2.0	17	1999
Vesijärvi (F)	11200	Mesotrophic	1.7-26.0	1.2-3.7	15	1994-99
Tuusulanjärvi (F)	610	Hypertrophic	7.8-67	0.3-0.9	13	1995-99
Verevi (E)	12.6	Hypertrophic	4.4-414	0.6-3.7	53	1994-99
Lohjanjärvi (F)	9400	Eutr./mesotr.	8.5-64	0.7-1.75	22	1997-99
Maardu (E)	170	Eutr./mesotr.	7.9-73	0.9-3.0	15	1999
Arbi (E)	4.5	Eutrophic	6.6-17.3	1.6-1.8	3	1994
Võrtsjärv (E)	27000	Eutrophic	25.0-102	0.15-1.0	22	1994-99
Ülemiste (E)	960	Eutrophic	23.1-121	0.5-3.6	46	1998-99
Enäjärvi, Vihti (F)	500	Eutrophic	5.0-5.2	1.0	3	1997
Keravanjärvi (F)	100	Humic	30-33	1.2	3	1997
Pääjärvi, Lammi (F)	1300	Humic	3.3-12.2	1.6-3.0	14	1994-99
Harku (E)	163.8	Dyseutrophic	74-895	0.1-0.4	46	1998-99
Uljaste (E)	60	Dyseutrophic	3.1-45	1.0-3.4	14	1994-96
Nohipalu Mustjärv	21.9	Dystrophic	1.7-46	0.4-0.9	15	1994-95

Table 2 – The main characteristics of the lakes in the FEI dataset. Minimum and maximum values of chlorophyll *a* concentration (C_{chl}), absorption coefficient of aquatic humus at 380 nm, and Secchi disc depth (z_{SD}) are from the measurements carried out in August 1997. All lakes are located in Finland.

Lake	Area, ha	Lake type	C_{chl} , $\mu\text{g l}^{-1}$	(z_{SD}) m	<i>n</i>
Puujärvi	700	Oligotrophic	1.5	7.0	6
Päijänne	7700	Oligotrophic	2.5	4.0	4
Iso-Kisko	700	Oligotrophic	2	4.0	8
Vesijärvi	11100	Mesotr.	12	2.9	4
Lohjanjärvi	9400	Eutr./mesotr.	10-55	0.8-2.9	18
Hiidenvesi	3000	Eutr./mesotr.	7-30	0.7-1.2	8
Kiskonjärvi	700	Eutrophic	50-100	0.5	10
Enäjärvi, Vihti	500	Eutrophic	38	1.0	6
Pääjärvi, Lammi	1300	Humic	6	2.7	3
Keravanjärvi	100	Humic	12	1.6	6

these concentrations were not measured by the EMI and the spectra of $c_f^*(\lambda)$ were determined with spectrophotometers of different measurement characteristics, the results of these two datasets are here analysed separately. The absorption spectrum studies were mainly based of the EMI dataset due to the large number of measurements. Some parts of the datasets have been earlier analysed by Mäekivi and Arst (1996) and Kallio (1999). Here we included new data and made more detailed analyses.

The lake type in the whole dataset ranged from oligotrophic to dyseutrophic/humic and the variation in size and depth was considerable (Tables 1 and 2). Some lakes (Lohjanjärvi and Hiidenvesi) consist of several sub-basins with trophic level varying from eutrophic to mesotrophic.

In the EMI dataset, most water samples were taken from the surface layer of 0-0.5 m, but some part (approximately 25%) from depths 2, 4 and/or 6 m. The expeditions were carried out repeatedly in 1994-1999 during the period from May to October. In the FEI dataset (Table 2), ten lakes were sampled in August while only six were surveyed in May 1997. The number of sampling stations per lake ranged from 2 to 12. All the samples were taken from the surface layer of 0-0.4 m. Sampling in May was carried out on 7th and 8th and in August on 11th, 12th and 18th.

Apparatus and Methods

In the EMI dataset the attenuation coefficient spectra of filtered water were measured with a spectrophotometer *Hitachi U1000*. In connection with the determination of truthful spectra of $a_{CDOM}(\lambda)$ numerous problems arise. The major problem is the quality of initial data, which can be influenced by a delay of the processing of water samples, technical characteristics of the spectrophotometer and properties of filters. The water samples were filtered through Millipore polycarbonate filters with

a pore size of 0.45 μm . We did not use filters of 0.22 μm because the water of many lakes was so rich in particles that it would have clogged up the fine filters. To estimate the error brought about by the filters of 0.45 μm pore size we carried out special experiments. The water samples from four lakes of different trophic state were taken and the water was filtered first through a 0.45 μm filter, and then through a 0.22 μm filter (Millipore, gray-coloured). The spectra of $c_f^*(\lambda)$ were measured after the first and the second filtering with a *Hitachi U1000*. For three eutrophic lakes (Ülemiste, Harku and Maardu) additional filtering brought about a slight decrease in the values of $c_f^*(\lambda)$ (on average by 3-4.5%). For oligotrophic Lake Paukjärv there was practically no difference between the results of two-filter and one-filter experiments.

In the FEI dataset, the values of $c_f^*(\lambda)$ were measured at the Tvärminne Biological Station with a Shimadzu UV-PC2101 spectrophotometer using a 5 cm quartz cuvette in May 1997, while in August the measurements were carried out in the Laboratory of Uusimaa Regional Environment Centre with a Perkin Elmer Lambda spectrophotometer using a 1 cm glass cuvette. The wavelength range in both measurements was 380-800 nm with an interval of 1 nm. Particulate material was removed from the water samples by filtering through a Nuclepore polycarbonate (pore size 0.4 μm) filter. Filtering was done within two days after sampling and absorption spectra were measured within a week after filtering. The long storing time between filtering and the absorption measurement may be a source of error. According to Karlsson *et al.* (1994) colloidal size range may change after filtering. On the other hand, Gege (1998, 2000) has pointed out that filtering may produce micro bubbles in the water. These micro bubbles attenuate light and influence on the absorption measurement results. They can be eliminated by storing the filtered water before the measurement. By our experiments (unpublished, carried out in EMI) the storing of water samples within a week or two in most cases (21 from 23) brings about the increase of $c_f^*(350)$ values from 2 to 10%.

Concentration of dissolved organic carbon was determined at the Laboratory of the Finnish Environment Institute. Organic carbon in the filtered water was oxidized to CO_2 and the concentration was determined by an infrared spectrometry measurement (EN1484, 1997). Before the measurement the inorganic carbon and volatile organic carbon were removed by acidification and purging.

Modelling of the Absorption Curve of CDOM

The absorption curve of CDOM was modelled by commonly used way, assuming its exponential dependence on the wavelength λ

$$a_{CDOM}(\lambda) = A \exp(-S\lambda) \quad (2)$$

which gives

$$a_{CDOM}(\lambda) = a_{CDOM}(\lambda_0) \exp(-S(\lambda-\lambda_0)) = a_{CDOM}^*(\lambda_0) C_{CDOM} \exp(-S(\lambda-\lambda_0)) \quad (3)$$

where A is a coefficient, $a_{CDOM}(\lambda)$ is the absorption coefficient of CDOM, λ_0 is the reference wavelength (usually it is between 360 and 420 nm), a^*_{CDOM} is specific absorption coefficient of CDOM, S is slope parameter, C_{CDOM} is the concentration of CDOM in the water. Obviously, the logarithm of the absorption coefficient of CDOM is a linear function of wavelength.

The correction for scattering by small residual particles and colloids that are not retained on the filter was determined by the widely used relationship

$$\beta(\lambda) \equiv c^*_{f}(\lambda_R) (\lambda_R/\lambda)^g \tag{4}$$

with $\lambda_R \gg \lambda_0$ being another reference wavelength in the red region of the spectrum, where it was assumed that $a^*_{CDOM}(\lambda_R)=0$.

Taking into account that $\chi = c^*_{f}$, Eqs. (1) and (4) give

$$c^*_{f}(\lambda) = a_{CDOM}(\lambda) + \beta \quad \text{and} \quad a_{CDOM}(\lambda) = c^*_{f}(\lambda) - c^*_{f}(\lambda_R) (\lambda_R/\lambda)^g \tag{5}$$

In the calculations performed by EMI three values of g were used: $g=0$ (by Gallie 1994), $g=1$ (by Davies-Colley and Vant 1987) and $g=2$ (by Aas 2000) (in FEI calculations $g=2$ was not considered). The value of λ_R was 700 nm (EMI) or 750 nm (FEI).

As seen from Eqs. (4) and (5), for determining truthful values of $a_{CDOM}(\lambda)$ the correct value of $c^*_{f}(\lambda_R)$ is needed. However, the maximum relative errors of c^*_{f} (instability of the spectral curve) are observed in the red and infrared regions of the spectrum, where the values of c^*_{f} are small. In order to diminish this error, the curves of $c^*_{f}(\lambda)$ in the region of $\lambda > 500$ nm were approximated with power functions in the EMI dataset. The value of $c^*_{f}(\lambda_R)$ was calculated applying the best fit in the least squares sense. In the FEI dataset the curves of $c^*_{f}(\lambda_R)$ measured in May were monotonously decreasing with increasing wavelength and there was no need to smooth them; for the August data the value of $c^*_{f}(\lambda_R)$ was determined by calculating the mean value from three wavelengths around 750 nm.

Next, we determined the correction $\beta(\lambda)$ for each wavelength of measurements and calculated the spectra of $a_{CDOM}(\lambda)$ by Eq. (5). As a result we obtained three different curves of $a_{CDOM}(\lambda)$ according to three values of g in Eqs. (4) and (5). Then the parameters of the exponential model (Eq. (2)) were determined for each value of g and for different lakes. Finally, the suitability of the exponent for describing spectra in different regions between 350 and 700 nm was estimated. Namely, the discrepancies between modelled (a_{CDOM}^{mod}) and measured (a_{CDOM}^{meas}) values were calculated using the exponential approximation in the ranges of 350-700, 350-500 and 380-500 nm.

We calculated also the values of standard deviation (σ) and mean relative error (M) for the whole data complex according to the following formulae

$$\sigma^2 = \frac{1}{n} \sum_{i=1}^n (a_{CDOM}^{mod}(\lambda_i) - a_{CDOM}^{meas}(\lambda_i))^2 \tag{6}$$

$$M = \frac{2}{n} \sum_{i=1}^n \frac{a_{CDOM}^{mod}(\lambda_i) - a_{CDOM}^{meas}(\lambda_i)}{a_{CDOM}^{mod}(\lambda_i) + a_{CDOM}^{meas}(\lambda_i)} \quad (7)$$

where n is the total number of a_{CDOM} measurements (all measured spectra, considering one after another the regions 350-700, 350-500 and 380-500 nm).

Other Methods of Modelling the Spectra of $a_{CDOM}(\lambda)$ and $c^*(\lambda)$

In addition to the commonly used exponential function we tried to analyse some other possibilities of modelling the absorption coefficient spectra of CDOM. Recently, Gege (2000) proposed a Gaussian model, based on a fundamental property of the absorption process, for absorption spectra of CDOM. Namely, in the case when the absorption lines are very narrow, have equal absorption probabilities and may be assumed statistically distributed, the envelope of the absorption lines is described by the probability density function of the Gaussian distribution

$$f(\lambda) = \exp \left\{ -\frac{1}{2} \left(\frac{\lambda - \lambda_j}{\Gamma_j} \right)^2 \right\} \quad (8)$$

The actual shape of the measured absorption spectra of CDOM is not particularly close to the Gaussian distribution. An attempt was made by Gege (2000) to approximate the actual spectra in the form of a superposition of a (small) number of Gaussian functions with different parameters. It was found that, generally, two or three Gaussian distributions are necessary in order to obtain reasonable accuracy of the approximation.

Although the described approach is highly interesting and the results are most promising, it also raises a number of questions. The traditional approximation contains three parameters (the absorption coefficient, the slope of the exponent and the reference wavelength) that are well investigated for many applications. Any of the Gaussian distributions also contains three parameters (an analogy to the absorption coefficient, reference wavelength and spectral width). Thus, approximation of the absorption spectra with a single Gaussian function reduces to determining as many parameters as in the classical case. If a superposition of two or three Gaussians is used, the number of parameters will double or triple. Optimization procedures in multi-dimensional parameter spaces frequently lead to serious mathematical problems (Dennis and Schnabel 1996). The measured absorption spectra are non-symmetric and their approximation with a superposition of symmetric Gaussian functions might not capture some of their important features. A conceptual question arises from the general philosophy of the approximation technique. The first approximation should capture the main part of the behaviour of a spectrum in question, and each subsequent additive in the (perhaps asymptotic) expansion is essentially smaller than the former ones (*e.g.* Nayfeh 1968). All the single Gaussians functions in (Gege 2000) are comparable in a relatively large spectral interval.

Both the traditional approximation (Eq. (2)) and the Gaussian distribution belong to a wider class of hyperexponential functions

$$w(\lambda) = W \exp(-\alpha \lambda^\eta) \tag{9}$$

representing the Weibull cumulative distribution function (WCDF) of the Weibull (Gnedenko) distribution. The traditional distribution in Eq. (2) corresponds to $\eta = 1$ and a Gaussian (centred at the origin) to $\eta = 2$. The use of a Gaussian would be justified if the parameter η were close to 2, at least within the most significant part of the spectra (e.g., in the range of 300-600 nm). For example, in meteorology the Weibull distribution is frequently replaced by the Rayleigh distribution (Mohr and Sandström 1996). An argument for considering the hyperexponent for describing a_{CDOM} is that generally it is asymmetric and resembles much more the actual spectra of a_{CDOM} . Some preliminary estimations of α and η relying on 30 measured spectra of a_{CDOM} and respective conclusions are presented later (Results obtained by other methods).

The above-described methods assume that the correction β can be determined from Eq. (4) with the use of the values of λ_R and $c_f^*(\lambda_R)$ in the red region of the spectrum. By our measurements, the spectra of $c_f^*(\lambda)$ in this region are often unstable, may contain significant relative errors, and may lead to unreliable values of β . In order to smooth the measured spectra of $c_f^*(\lambda)$ and to obtain an optimal value of β , the right-hand side of Eq. (5) was (somewhat untraditionally) approximated as a sum of exponential and power functions as follows

$$c_f^*(\lambda) = C_1 \exp(-C_2 \lambda) + \frac{C_3}{\lambda^g} \tag{10}$$

where the parameters C_1 , C_2 and C_3 were determined using the classical least squares method. The first term in the right-hand side of Eq. (10) can be considered equivalent to the classical representation of the spectrum of a_{CDOM} in Eq. (2). However, practical calculations show that the second term, C_3/λ^g , is numerically not equal to β obtained by Eq. (5), but it behaves to some extent similarly (both are inversely proportional on λ). In what follows only the value $g = 1$ was used.

The problem of determining the best fit of $c_f^*(\lambda)$ in the three-parameter space (C_1 , C_2 , C_3) was solved applying two different methods. As the exponential term in Eq. (10) is very small in the range of 600-700 nm, a suitable initial value for C_3 is, in fact, $C_3 = f_i \lambda_i$, where f_i is any measured value of c_f^* in this range. The average of $f_i \lambda_i$, $600 \leq \lambda_i \leq 700$ nm, was also reasonable. In the range of smaller wavelengths, the exponential term in Eq. (10) is dominating and it may be assumed that $c_f^*(\lambda) \approx C_1 \exp(-C_2 \lambda)$. The initial values of C_1 and C_2 were found with the use of measured values of $c_f^*(\lambda)$ at $\lambda_1 = 500$ nm and $\lambda_2 = 600$ nm from the following system of equations

$$f(\lambda_1) = C_1^0 \exp(-C_2^0 \lambda_1) \quad f(\lambda_2) = C_1^0 \exp(-C_2^0 \lambda_2) \tag{11}$$

which yields

$$C_1^0 = f(\lambda_1) \exp(C_2^0 \lambda_1) \quad C_2^0 = \{\ln f(\lambda_1) - \ln f(\lambda_2)\} / (\lambda_2 - \lambda_1) \quad (12)$$

Since the secant method for solving nonlinear systems showed certain instability with respect to the initial values of the iteration-process, the coordinate-wise descent method was mostly used.

Results and Discussion

Variability of CDOM in Estonian and Finnish Lakes

As noted above, the amount of CDOM in water bodies can be characterized by its absorption coefficient in the UV or blue part of the spectrum. We chose the wavelength 380 nm. The minimal, maximum and mean values of $a_{CDOM}(380)$ for lakes described in Tables 1 and 2 are shown in Tables 3 and 4. There are rather significant differences in and between the lakes, minimum values varying from 0.71 to 17.3, maximum from 1.91 to 19.5 and mean values from 1.25 to 18.4. The standard deviations vary too, but their values are influenced not only by the variation of CDOM, but also by the number of measurements (if there are only 2-3 measured spectra then σ is usually smaller than in the case of 10 or more spectra).

Lake Nohipalu Mustjärv is very different from other lakes due to its extremely high concentration of CDOM and we cannot apply the usual methods when analysing the results of spectrophotometric measurements of water samples. For this reason data of Lake Nohipalu Mustjärv are left out from our statistical analyses. The minimum and maximum values of $a_{CDOM}(380)$ for N. Mustjärv measured in ice-free period during 1994-1995 were respectively 38 and 93 m^{-1} . Thus, the minimum is 2-50 and maximum 5-76 times as high as the values shown in Tables 3 and 4. The value of c_f^* (700) for N. Mustjärv is around 1.5-2 m^{-1} , which is also considerably higher than the relevant value for the other lakes. The assumption that a_{CDOM} in the region of 650-750 nm is equal to zero is not valid in case of N. Mustjärv. Consequently, we cannot, relying on $a_{CDOM}(\lambda_R)$, calculate the correction β using Eq. (4) and the spectrum of $a_{CDOM}(\lambda)$ by Eq. (5). The typical value of S for N. Mustjärv, determined without any correction, ranges from 0.010 nm^{-1} (interval 350-700 nm) to 0.013 nm^{-1} (intervals 350-500 and 380-500 nm). To determine S with corrections data of a_{CDOM} somewhere between 750 and 900 nm are needed. However, as known, the $a_{CDOM}(\lambda)$ spectra in the range of 730-900 nm are sensitive to the temperature difference between the samples of filtered and distilled water (Gege 1998, 2000). Therefore, the values of $c_f^*(\lambda_R)$ in the range of $\lambda > 750$ nm have to be measured very carefully. Obviously, strongly dystrophic lakes such as N. Mustjärv are worth special investigation, with the spectra of c_f^* measured up to 800-900 nm and the amount of DOC as well as specific absorption coefficient spectra of CDOM determined.

Table 3 – Minimum, maximum and mean values of $a_{CDOM}(380)$ in m^{-1} , and respective values of standard deviation (σ , in m^{-1}) for the EMI dataset ($g=1$, $\lambda_R=700$ nm). The lakes are described in Table 1

Lake	Min	Max	Mean	σ	n
Arbi (E)	3.97	5.15	4.58	0.590	3
Enäjärvi, Vihti (F)	2.53	2.63	2.56	0.058	3
Harku (E)	8.38	19.5	13.6	3.91	46
Keravanjärvi (F)	17.1	18.1	17.7	0.507	3
Koorküla Valgjärv (E)	1.14	2.55	1.75	0.347	20
Kurtna Nõmmjärv (E)	1.93	7.52	4.27	1.80	13
Linajärv (E)	7.32	12.4	10.1	1.65	17
Lohjanjärvi (F)	4.98	14.6	9.24	3.59	22
Maardu (E)	4.06	8.1	5.82	1.53	15
Nohipalu Valgjärv (E)	1.69	5.96	3.22	1.05	37
Pääjärvi, Lammi (F)	7.77	12.7	10.8	1.32	14
Päijänne (F)	3.62	5.08	4.48	0.051	10
Paukjärv (E)	0.71	4.09	1.25	0.680	21
Puujärvi (F)	1.66	1.91	1.79	0.177	2
Tuusulanjärvi (F)	6.05	13.2	10.8	2.32	13
Uljaste (E)	3.62	9.61	5.61	1.56	14
Vesijärvi (F)	1.86	7.91	2.98	1.45	15
Verevi (E)	4.16	13.6	5.85	1.81	53
Võrtsjärv (E)	3.68	17.3	8.27	3.83	22
Ülemiste (E)	4.33	9.09	6.61	1.10	46
All	0.71	19.5	6.56	1.47	389

Table 4– Minimal, maximal and mean values of $a_{CDOM}(380)$ in m^{-1} ($g=1$, $\lambda_R=750$ nm), respective values of standard deviation (σ , in m^{-1}) and the number of measurements (n) in the FEI dataset. The lakes are described in Table 2.

Lake	Min	Max	Mean	σ	n
Puujärvi	1.73	2.70	2.19	0.46	6
Päijänne	3.39	3.57	3.48	0.08	4
Iso-Kisko	2.09	3.28	2.67	0.52	8
Vesijärvi	1.91	1.95	1.93	0.02	4
Lohjanjärvi	3.61	11.87	6.31	2.06	18
Hiiðenvesi	6.44	8.18	7.79	0.57	8
Kiskonjärvi	6.93	10.67	8.45	1.44	10
Enäjärvi, Vihti	2.74	5.44	4.01	1.16	6
Pääjärvi	10.17	10.46	10.33	0.15	3
Keravanjärvi	17.26	19.34	18.45	0.80	6
All	1.73	19.34	6.61	4.48	73

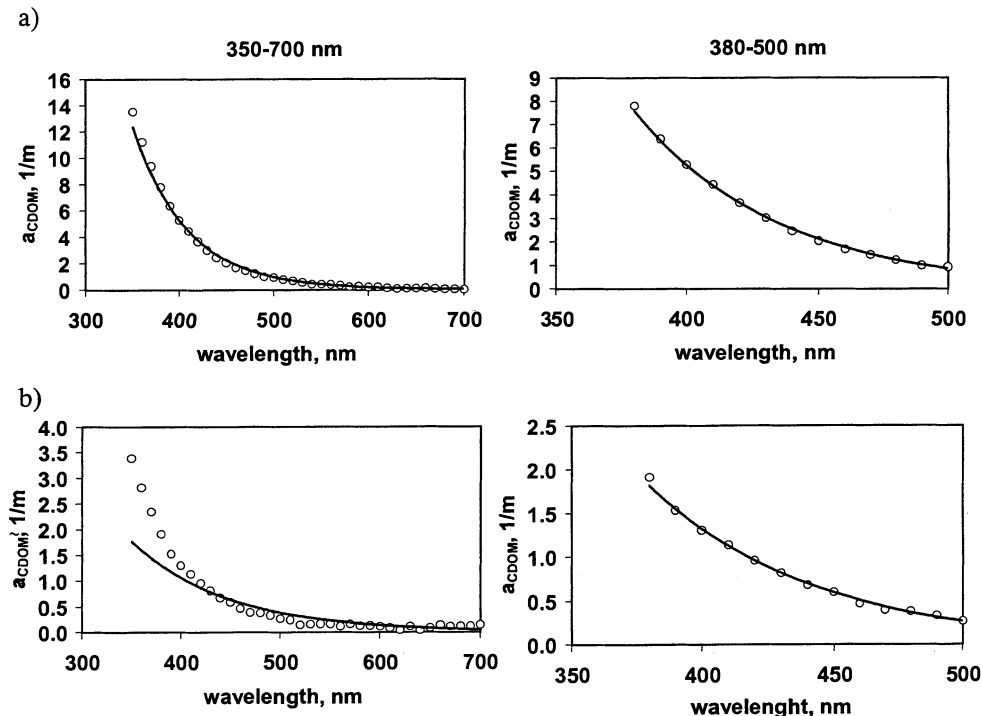


Fig. 1. Suitability of the exponent function for the approximation of a_{CDOM} curves in dependence of spectral range (350-700 and 380-500 nm). Examples are presented for: (a) Lake Verevi (17.06.99) and (b) Lake Puujärvi (12.08.97).

Exponential Approximation in Different Spectral Regions

As said before, for the spectra of $a_{CDOM}(\lambda)$ calculated by Eq. (5) the exponential approximation was determined considering several intervals in the region of 350-700 nm. In some cases the curve of a_{CDOM} derived from measurements coincided well with exponential approximation in the whole range of 350-700 nm as well as in the ranges of 350-500 and 380-500 nm (example in Fig. 1a), but in many cases the suitability of exponent was significantly worse for the whole region than for its smaller parts (example in Fig. 1b).

We computed also spectral relative differences, $r(\lambda)$, for separate a_{CDOM} curves, using Eq. (7) with $n=1$. A characteristic picture of $r(\lambda)$ and corresponding spectral absolute differences are presented in Fig. 2. As we can expect, the greatest relative differences occur in the red region of the spectrum, due to very small a_{CDOM} values at these wavelengths (the corresponding absolute differences are also small). The main reason of irregular variation of a_{CDOM} between 600 and 700 nm is the instability of spectrophotometric results in this region (the values of $c^*_f(\lambda)$ differ only slightly from those of distilled water). The rather high values of $r(\lambda)$ between 350 and 400

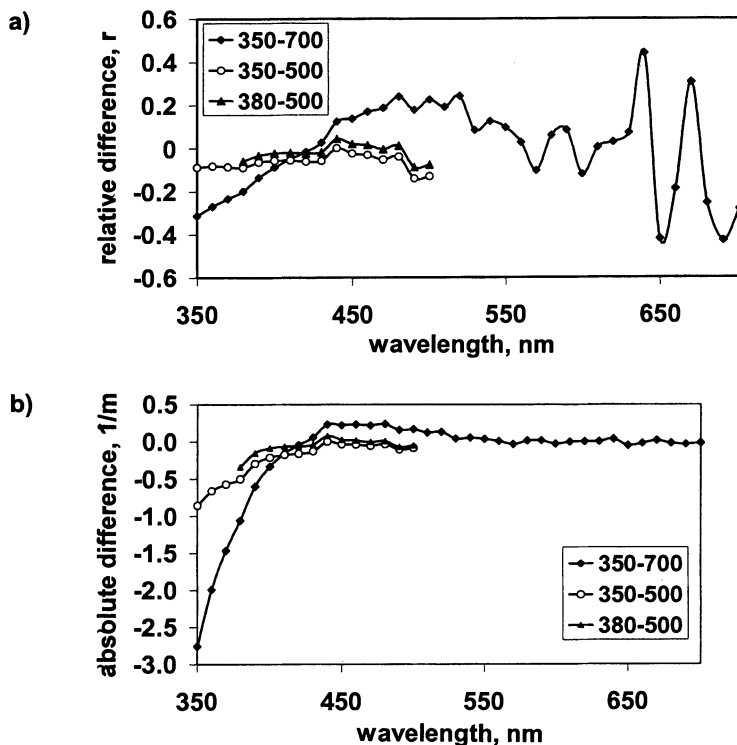


Fig. 2. Comparison of the values of relative and absolute differences ($(a_{CDOM}^{meas}(\lambda_i) - a_{CDOM}^{mod}(\lambda_i))$) between measured and modelled values of a_{CDOM} , relying on exponent approximation for different regions of the spectrum (Lake Verevi, 17.06.1999).

nm indicate substantial absolute differences in this interval (curve 350-700 nm in Fig. 2). In the case of using exponential approximation only in the spectral interval 350-500 or 380-500 nm the values of $r(\lambda)$ are small. Typically absolute differences are great in the violet and blue regions of the spectrum.

The suitability of the exponent function for modelling the CDOM absorption coefficient spectra can be estimated determining the values of standard deviation and mean relative difference (Eqs. (6) and (7)). The results obtained are presented in Table 5. As we can see the values of σ and M for the whole PAR region (350-700 nm) are markedly higher than those for the regions of 350-500 and, especially, of 380-500 nm. Comparison of the data obtained from 389 spectra and 100 spectra (Table 5) for the same spectral intervals and same values of g show that 100 spectra are not sufficient for describing the differences between measured and modelled spectra: the values of s in case of 389 spectra are 1.9-2.3 times higher and M 2-15 times lower than those in case of 100 spectra. Using the correction with $g=2$ we obtain only slightly smaller values of σ than in the case of $g=1$, but higher values of M (Table 5).

Optical Properties of Dissolved Organic Matter in Lakes

Table 5– Standard deviation σ and mean relative difference M calculated using different corrections and spectral intervals in the EMI dataset

$\Delta\lambda$, nm	Data of 1994-1999 (389 spectra)				Data of 1999 (100 spectra)				
	350-700	350-500	380-500	380-500	350-500	380-500	380-500	350-500	380-500
Type of correction	$g=1$	$g=1$	$g=1$	$g=0$	$g=1$	$g=1$	$g=0$	$g=2$	$g=2$
σ , m^{-1}	9.632	2.066	0.982	1.997	0.8951	0.5206	1.0630	0.8121	0.4322
M	0.0614	0.0056	0.0011	0.0081	0.0177	0.0172	0.0168	0.0184	0.0179

Values of Slopes

Applying Eqs. (2), (4) and (5) we modelled all our spectra obtaining the values of slope S . The mean values of S for each lake determined for different spectral intervals and using different values of g are presented in Table 6. The minimum values of slope S were observed for the region 350-700 nm, while the regions 350-500 and 380-500 nm gave more or less identical slopes. All values of S calculated without any correction are smaller than the respective S values determined with various corrections. We can also see that application of the value $g=2$ in Eq. (4) brings about a slight increase (2-3%) of S .

In the FEI dataset, we found a drop of some absorbances at wavelengths shorter than 385 nm in the August data. This discontinuation of the exponential curve was probably due to the fact that a glass-cuvette was used. Therefore, wavelengths shorter than 385 nm were omitted from the absorption data measured in August. The wavelength range used for the slope estimation was 385-500 nm. Slopes are shown in Table 7. In the whole FEI dataset the minimum and maximum slope parameters S ($g=0$) were 0.0124 and 0.0196 nm^{-1} , respectively.

The variation of S (determined by data of measurement series for each lake) is shown in Fig. 3. We can see that in some lakes (mostly clear-water lakes) the differences between minimum and maximum values of S are significant. Small variability of S can be the real characteristic of the lake (probably for Lammi Pääjärvi, Linajärv, Maardu, Harku, Ülemiste), but sometimes it is hard to draw conclusions due to the small number of measurements (Keravanjärvi, Arbi, Enäjärvi).

The values of S obtained by us for different values of g and different spectral intervals are within the limits of S cited by Aas (2000), from 0.004 to 0.053 nm^{-1} . Our values are from 0.006 to 0.03 nm^{-1} , the mean values computed for each lake varying within the range of 0.012-0.020 nm^{-1} (with corrections) or from 0.008 to 0.018 nm^{-1} (without correction). The mean value of S obtained relying on all our data varies from 0.011 nm^{-1} (interval 350-700 nm without correction) to 0.018 nm^{-1} (interval 350-500 nm in case of $g=2$, Tables 6 and 7). As mentioned before, values of S similar to our values have been presented in earlier publications by different authors. In Bricaud *et al.* (1981) S varies from 0.10 to 0.20 (mean value 0.14). These values are consistent with the absorption curve published by Jerlov (1968)

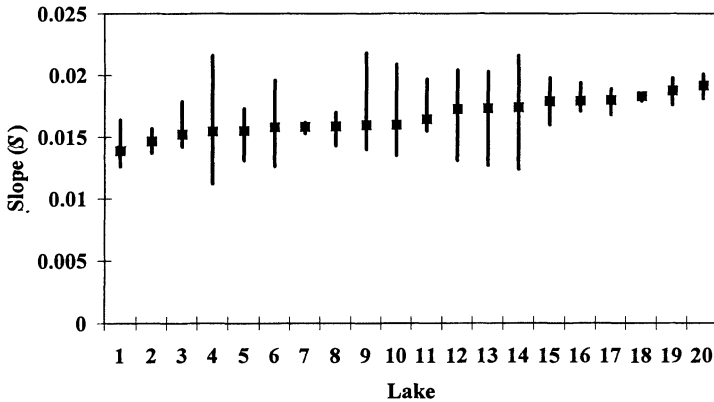


Fig. 3. The average, minimum and maximum values of the slope S in different lakes calculated for spectral interval 380-500 taking $g=1$ (EMI dataset). The number of measurements used for each lake is shown in brackets: 1-Tuusulanjärvi (13), 2-Linajärv (17), 3-Päijänne (10), 4-Nohipalu Valgjärv (37), 5-Lohjanjärvi (22), 6-Uljaste (14), 7-Keravanjärvi (3), 8-Lammi Pääjärvi (14), 9-Kurtna Nömmjärv (13), 10-Vesijärvi (15), 11-Vörtsjärv (22), 12-Paukjärv (21), 13-Verevi (53), 14-Koorküla Valgjärv (20), 15-Puujärvi (2), 16-Arbi (3), 17-Harku (46), 18-Enajärvi (3), 19-Ülemiste (46), 20-Maardu (15).

Table 6 – Variability of mean values of S (nm^{-1}), calculated by each lake separately for different spectral intervals and with different corrections (EMI dataset, $\lambda_R = 700 \text{ nm}$)

$\Delta\lambda$, nm	g	Min	Max	Mean
350-700	1	0.012	0.017	0.0139
350-500	1	0.013	0.019	0.0171
380-500	1	0.014	0.019	0.0171
380-500	0	0.013	0.018	0.0160
350-700	–	0.008	0.017	0.0105
350-500	–	0.012	0.019	0.0150
380-500	–	0.012	0.018	0.0143
350-500	2	0.016	0.020	0.0183
380-500	2	0.015	0.019	0.0179

Table 7 – Mean values of slope S (nm^{-1}) determined for the spectral interval 380-500 nm using corrections ((Eq.4)) with $g=1$ and $g=0$, and also without any correction in the FEI dataset. The reference wavelength (λ_R) was 750 nm. σ = standard deviation.

Month	n	$S(g=1)$		$S(g=0)$		S (no correction)	
		Mean	σ	Mean	σ	Mean	σ
May	26	0.0177	0.00194	0.0162	0.00084	0.0140	0.00108
August	47	0.0169	0.00192	0.0157	0.00099	0.0139	0.00129
May & August	73	0.0171	0.00193	0.0159	0.00095	0.0140	0.00121

($S=0.015$), with Lundgren's (1976) data for Baltic waters (S is between 0.011 and 0.017), and also with Kirk's (1976) data for lake waters, which lead to values of S between 0.013 and 0.016 nm^{-1} . However, the results obtained later show somewhat higher values of S . Davies-Colley and Vant (1987) reported the mean slope of S of 0.0187 nm^{-1} (± 0.0013) in twelve freshwater lakes in New Zealand. Effler *et al.* (1991), carrying out investigations for the waters of Lake Ontario, obtained S varying in the range of 0.0159-0.0206, the average value being 0.0170 nm^{-1} . Hoge *et al.* (1993) obtained the mean value of 0.018 nm^{-1} , S varying from 0.015 to 0.023 nm^{-1} . Mäekivi and Arst (1996) and Kallio (1999) using $g=1$ recommended the mean value $S=0.017$. Strömbeck and Pierson (2001) reported the mean slope of 0.0151 (range 0.0135–0.0201) for Swedish lakes. Aas (2000), who suggested to use $g=2$, obtained respective S varying between 0.020 and 0.024. We found no connection between the values of S and $a_{CDOM}(380)$ or between S and the lake type; there are no regular seasonal changes of S (analogous conclusions were made by Bricaud *et al.* 1981). The detailed analysis on how the optical properties of CDOM depend on lake (*e.g.* morphology, retention time) and catchment characteristics (vegetation, source of organic carbon) was not possible to carry out due to lack of data. However, these factors are often typical to a certain lake type (eutrophic lakes are normally shallow and have a short retention time, oligotrophic lakes are deep and humic lakes are characterized by a high load of allochthonous organic carbon). The deeper analysis of these connections is undoubtedly necessary, but it needs a special investigation with a big amount of additional data.

Results Obtained by Other Methods

We analysed the values of a and η in Eq. (9) for a number of spectra (30) measured in 13 lakes. Parameters of a WCDF expressed as a function $w(C, \alpha, \eta, \lambda) = C \exp(-\alpha\lambda\eta)$ were estimated in the spectral interval 350-700 nm. The best fit in the three-dimensional parameter space (C, α, η) was sought as the global minimizer of the difference between measured spectra and the fit in the least-squares sense without any additional bounds or constraints. However, here we have to remember that (as was shown by Gege (2000) and in FEI measurements) the actual curve of a_{CDOM} has a maximum around 200 nm and we have no data on its behaviour when approaching to $\lambda = 0$. The data on a_{CDOM} mostly needed are between 300 and 800 nm (our measurement results were in the range of 350-700 nm).

Indeed, it turned out that only 50% of the 30 spectra under investigation gave the optimum value of η provided the coefficient C remains bounded. In almost all the cases when the optimum was reached, the value of η was below 1 (typically between 0.5 and 0.7) and only in one case it was 1.35. This result is not surprising since the majority of the measured absorption coefficient spectra are concave curves in the semilogarithmic co-ordinates and hyperexponential functions are concave curves if $\eta < 1$, straight lines in the case of traditional approach $\eta = 1$ and convex curves provided $\eta > 1$. All our spectra with an optimal value of η gave an excellent fit when we

used for approximation a single hyperexponent: the values of standard deviation of different spectra vary between 0.036 and 0.91 m⁻¹ and mean relative differences between 0.0077 and 0.0021. We calculated also the “absolute values of relative errors”, M_1 , relying on absolute values of differences between measured and modelled $a_{CDOM}(\lambda)$ in Eq.(7), the results obtained are in the range 0.048-0.36. The main factor increasing the values of M_1 is high relative differences in the long-wave region (where the measured spectrum of a_{CDOM} often shows irregular behaviour), obviously, these differences are caused by measurement errors of $a_{CDOM}(\lambda)$ and not by the unsuitability of the method. These results suggest that use of methods based on hyperexponential functions with the exponent η below 1 rather than the Gaussian distribution can be more effective for describing the features of actual spectra of a_{CDOM} .

However, for almost 50% of the spectra it was found that no best fit of absorption coefficient spectra with the hyperexponential function in the least-squares sense exists at all. For those spectra, the exponent η tends to zero and the coefficient $C = w|_{\lambda=0}$ to infinity. Analogous situations frequently occur in multidimensional non-linear unconstrained optimization problems where a global minimizer is sought (Dennis and Schnabel 1996). This feature suggests that the use of an even larger number of parameters is evidently not justified unless there are sound physical reasons for additional constraints. Note that the values of standard deviation obtained for cases without optimal solution mostly exceed those with optimal solution, but relative differences are rather similar for both cases.

The frequent occurrence of a “non-optimal” situation suggests that the behaviour of the function $w(C, \alpha, \eta, \lambda)$ should be studied in detail since a local minimizer might exist within suitably chosen bounds. A promising idea seems to be to seek the best fit only for wavelengths $\lambda > \lambda_1$ (λ_1 is, taking into account the physical grounds, some reference wavelength located between 220 and 300 nm) and its behaviour for smaller wavelengths than λ_1 is unimportant. Following this concept, the generalization of the hyperexponential functions $w(C, \alpha, \eta, \lambda_1, \lambda) = C \exp(-\alpha(\lambda - \lambda_1)\eta)$ might be a good approximation of the CDOM absorption coefficient spectra. Notice that this expression is a direct generalization of the Gaussian model of Gege (2000) represented by Eq. (8). Since this approximation contains already four parameters, a feasible way could be to fix the reference wavelength λ_1 on the basis of physical arguments. For a comprehensive analysis of the efficiency of this approximation, comparison of a large amount of measured and modelled spectra is needed and we hope to publish the respective results in the future.

The calculations by Eqs. (9)-(11) were performed using initial data (17 spectra of $c_f^*(\lambda)$) for 8 Estonian and Finnish lakes of different trophic state (included in Table 1). The variability of C_1 was significant (from 1.4×10^3 for clear-water Lake Paukjärvi to 36×10^3 m⁻¹ for humic Lake Lammi Pääjärvi). The coefficient C_2 was rather stable, varying in the limits from 0.0194 to 0.0219 nm⁻¹. Comparison of these values with S (Tables 6–7) shows that C_2 exceeds the relevant values of S , being

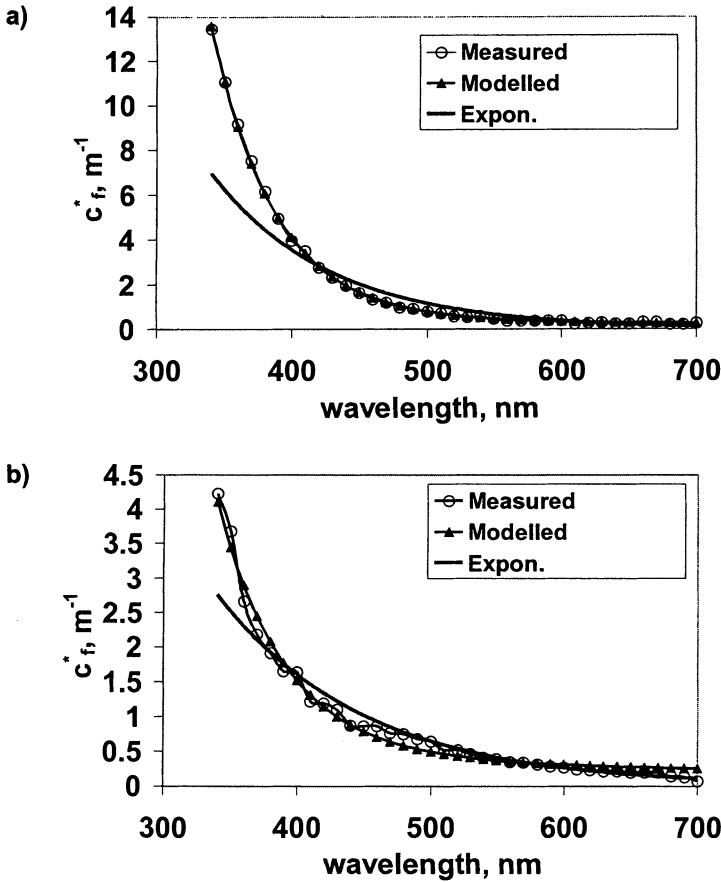


Fig. 4. Comparison of measured and modelled (Eq.10) and exponential approximation curves of $c_f^*(\lambda)$ for Lake Vörtsjärv (Sept.1994) and Lake Nohipalu Valgjärv (Aug. 1998).

closest to S when it is obtained using $g=2$ (Table 6). The ratio C_3/λ is formally equivalent to β (Eq. (4)), *i.e.* when $\lambda=700$ nm, then C_3/λ is comparable to $c_f^*(700)$. The correlation coefficient between these two parameters is 0.96, the regression formula is: $c_f^*(700) = 0.91C_3/700 - 0.05$. In most cases $C_3/700$ exceeds $c_f^*(700)$; thus, supposing that $C_1 \exp(-C_2\lambda)$ is equivalent to $a_{CDOM}(\lambda)$ we usually obtain somewhat smaller absorption coefficients than in the case of using Eqs. (2) and (3). However, actually the main objective of this method was not to determine the best fit for a_{CDOM} , but for $c_f^*(\lambda)$. The respective efficiency of the method was estimated calculating the values of standard deviation and mean relative error (analogously to Eqs. (6) and (7)) separately for each spectrum. The results obtained show that σ varies from 0.027 to 0.208 m^{-1} , M between -0.0082 and 0.109 and $M(abs)$ between 0.040

and 0.255 (the last figures were obtained using the absolute values of the difference ($c_f^*(\text{mod}) - c_f^*(\text{meas})$). The efficiency of this method for smoothing the curves of $c_f^*(\text{meas})$ is demonstrated also in Fig. 4a,b. It shows also that curves by Eqs. (9-11) give significantly better fit with measured curves than exponential approximation.

Specific Absorption Coefficient of CDOM

Before the calculation of the specific absorption coefficient of CDOM, $c_f^*(385)$ was plotted against the DOC concentration (Fig. 5.). As can be seen, some DOC seems to be left in the water at very low absorption values if a linear relationship between DOC and $c_f^*(385)$ is assumed. This residual DOC that is not optically active (*i.e.* does not absorb light) can be due to 1) colourless DOC in the original sample or 2) contamination during the process of analysing. One contamination source can be leaching of carbon from the Nuclepore polycarbonate-filter, which would lead to overestimation of DOC concentration. To find out the amount of carbon that could possibly be leached from the filter, ultra-purified (reverse osmosis, ion exchange and filtering) water was filtered after every fourth sample and the DOC concentration was determined. The DOC concentration of the purified water was higher than the detection limit of 0.5 mg L⁻¹ only in one case. However, when filtering the actual lake samples, the filter can be a bigger source of carbon due to the lengthening of the filtering time because of the particles retained on the filter.

Coloured dissolved organic carbon (CDOC) was estimated from the DOC results by

$$CDOC = DOC - C_0 \quad (13)$$

where C_0 is the concentration of colourless DOC. C_0 was obtained by calculating the intercept of the regression line on the DOC-axis separately for the two seasons (Fig. (5)). C_0 for May was 2.68 and for August 4.06 mg L⁻¹.

In order to be able to compare the results with other similar studies, the concentration of CDOM had to be estimated. CDOM was obtained through multiplying CDOC by 2 (assuming that the carbon content of the organic matter is 50%). The specific absorption coefficient $a_{CDOM}^*(\lambda_0)$ in L mg⁻¹ m⁻¹ was thereafter calculated by

$$a_{CDOM}^*(\lambda_0) = a_{CDOM}(\lambda_0) / CDOM \quad (14)$$

where $a_{CDOM}(\lambda_0)$ is the absorption coefficient of CDOM at wavelength λ (m⁻¹); CDOM is the concentration of CDOM (mg L⁻¹).

The specific absorption coefficient was calculated for 380 nm, because we wanted to compare our results with those published in the literature. As the quality of the absorption measurements between 380 and 385 nm in August was poor, the absorption coefficient at 380 nm was calculated from the absorption coefficient at 385 nm using the slope parameter of 0.0159 and Eq. (2). We also calculated the specific absorption coefficient for DOM.

Optical Properties of Dissolved Organic Matter in Lakes

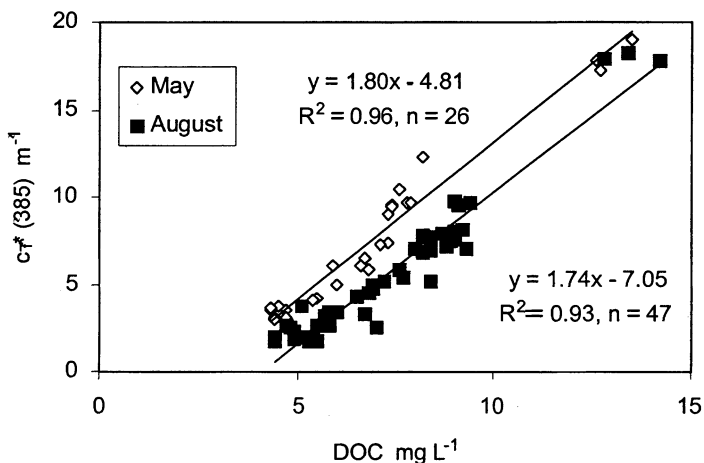


Fig. 5. Correlation between $c^*_f(385)$ and DOC concentration in FEI dataset in May and August 1997.

The mean specific absorption coefficient of CDOM of all the 73 samples was 1.01 L mg⁻¹ m⁻¹ (Table 8). The specific absorption coefficient of DOM was considerably lower (its mean value was 0.44 L mg⁻¹ m⁻¹, Table 8) due to the high proportion of non-absorbing material in DOM. The seasonal differences of the specific absorption coefficients were small (Table 8).

The mean specific absorption coefficient obtained in this study ($a^*_{CDOM}(380) = 1.01$ L mg⁻¹ m⁻¹) is higher than in most of the estimations published in the literature. In a review made by Baker and Smith (1982), including results from five different studies of the ocean and coastal waters, $a^*_{CDOM}(380)$ is in one case 2.16 L mg⁻¹ m⁻¹, but ranges in the rest of the studies between 0.25 and 0.565 L mg⁻¹ m⁻¹. Geographically the closest region to our lakes in this review is the Baltic Sea, for which Højer-slev (1980) obtained the value 0.565 L mg⁻¹ m⁻¹ based on the data of Nyquist (1979). However, in most of these studies the optically active part of DOM was not determined. Therefore, the literature data should probably be compared with $a^*_{CDOM}(380)$ of our data (mean: 0.44 L mg⁻¹ m⁻¹). This value is close to most of the specific absorption coefficients published in the literature. The specific absorption coeffi-

Table 8 – Specific absorption coefficient of CDOM and DOM (L mg⁻¹ m⁻¹) at 380 nm in the FEI dataset. Absorption coefficient was corrected with $g=0$ and $\lambda_R=750$ nm

Sampling time	$a^*_{CDOM}(380)$					$a^*_{DOM}(380)$				
	<i>n</i>	Mean	Min	Max	σ	Mean	Min	Max	σ	
May	26	0.92	0.74	1.14	0.12	0.53	0.32	0.77	0.15	
August	47	1.06	0.47	2.97	0.47	0.39	0.18	0.74	0.14	
May & August	73	1.01	0.47	2.97	0.40	0.44	0.18	0.77	0.16	

cient may be different in lakes than in seawater e.g. due to the high portion of allochthonous CDOM in lakes. Unfortunately, the studies on $a_{CDOM}(\lambda)$ in lakes have usually not included the determination the CDOM concentration that is needed in the calculation of specific absorption coefficient.

Conclusions

- 1) The total content of CDOM in Estonian and Finnish lakes was expressed by means of the absorption coefficient a_{CDOM} at the wavelength of 380 nm. The coefficient varied significantly, from 0.71 to 19.5 m^{-1} , the mean value (by all investigated lakes) being around 6.6 m^{-1} .
- 2) Application of the exponential function for the modelling of the spectrum of a_{CDOM} can give higher or lower correspondence between measured and modelled values depending on the spectral range and on the value g in correction β . This correspondence was estimated by means of standard deviation and mean relative difference. Their highest values occurred when the spectral interval was 350-700 nm; the smallest σ corresponds to the interval 380-500 nm and $g=2$, the smallest M to the same interval, but $g=1$.
- 3) The slopes of the exponential approximation varied widely, from 0.006 to 0.03 nm^{-1} (by literature data in the range of 0.004-0.053 nm^{-1}). The mean values of the slopes in Estonian and Finnish lakes vary in the range of 0.012-0.020 nm^{-1} (with several variants of corrections) and 0.008-0.018 nm^{-1} (without correction). Note that averaged over all lakes values for the interval 380-500 nm obtained from the EMI dataset are equal to those obtained from the FEI dataset (0.017 if $g=1$, 0.016 if $g=0$ and 0.014 without correction). These results are in good correspondence with most published and accepted data.
- 4) The slope values determined in different measurement campaigns can vary significantly for some lakes, but only slightly for others. There is no regularity connected with season or limnological type of lake.
- 5) The modelling of a_{CDOM} spectra by superposition of Gaussian functions (Gege 2000) probably allows a good description of the a_{CDOM} curve in a wide range of the spectrum. However, the necessary optimization procedures in multi-dimensional parameter spaces frequently lead to serious mathematical problems, especially when measurement data are available only for the PAR region (or its part), *i.e.* the data around the curves maximum are missing.
- 6) Attempts to describe the a_{CDOM} spectra in the region of 350-700 nm by means of hyperexponential functions ($\sim \exp(-\alpha\lambda^\eta)$) show that : (1) $\eta < 1$ (in the case of traditional exponential approximation $\eta=1$); (2) a promising idea is to seek the best fit only for wavelengths $\lambda > \lambda_1$, where λ_1 will be chosen on physical grounds.
- 7) The differences between derived from measurements and modelled a_{CDOM} curves are partly caused by measurement errors of the attenuation coefficient curve of

filtered water (especially in the red the region of the spectrum). It leads to the necessity to smooth the measured curve. We succeeded in approximating the attenuation coefficient curve of filtered water as a sum of exponent and power functions, where the corresponding parameters were determined using the classical least squares method.

- 8) The mean value of $a^*_{CDOM}(380)$ obtained in this study ($0.44 \text{ L mg}^{-1} \text{ m}^{-1}$) is close to the values published in the literature, if we assume that the specific absorption coefficient is calculated using DOM. The optically non-active fraction of DOM in our study was high and therefore $a^*_{CDOM}(380)$ was considerably higher ($1.01 \text{ L mg}^{-1} \text{ m}^{-1}$) than $a^*_{CDOM}(380)$. Usually CDOM has not been separated from DOM in the absorption studies and therefore comparison of the specific absorption coefficient of CDOM obtained for other regions could not be made.

Acknowledgements

The authors are indebted to the Estonian Science Foundation (Grants No 252, 1804, 3613) and to the Academy of Finland for financial support to this investigation. Jukka Seppälä from the Finnish Environment Institute and Satu Vuolas from the Uusimaa Regional Environment Centre are acknowledged for making the absorption measurements of the FEI dataset. The research carried out at the Finnish Environment Institute was partly funded by the Satellite Remote Sensing for Lake Monitoring (SALMON) Project (European Union, ENV4-CT96-0311).

References

- Aas, E. (2000) Spectral slope of yellow substance: problems caused by small particles. Proc. of the XV Conference of Ocean Optics, Monaco, 8 pp. (CD-ROM)
- Aiken G.R. (1988) A critical evaluation of the use of macroporous resins for the isolation of aquatic humic substances. In: Frimmel, F.H. and Cristman, R.F. (eds.), *Humic substances and Their Role in the Environment*, J.Wiley and Sons Ltd., pp. 15-18.
- Baker, K.S, and Smith, R.C. (1982) Bio-optical classification and model of natural waters, *Limnol. Oceanogr.*, Vol. 27,(3), pp. 500-509.
- Blough, N.V., Zafiriou, O.C., and Bonilla, J. (1993) Optical absorption spectra of waters from the Orinoco River outflow: Terrestrial input of colored organic matter to the Carribean, *J. Geophys. Res.*, Vol. 98, pp. 2271-2278.
- Bricaud, A., Morel, A., and Prieur, L. (1981) Absorption by dissolved organic matter of the sea (yellow substance) in the UV & visible domains, *Limnol. Oceanogr.*, Vol. 26, (1), pp. 43-53.
- Bukata, R.P., Burton, J.E., and Jerome, J.H. (1983) Use of chromaticity in remote measurements of water quality, *Remote Sensing Environ.*, Vol. 13, pp. 161-177.
- Carder, K.L., Steward, R.G., Harvey, G.R., and Ortner, P.B. (1989) Marine humic and fulvic acids: Their affects on remote sensing of ocean chlorophyll, *Limnol. Oceanogr.*, Vol. 34, pp. 68-81.

- Dera J. (1992) *Marine Physics*, PWN, Warszawa, Elsevier, Amsterdam, 516 p.
- Davies-Colley, R.J (1983) Optical properties and reflectance spectra of 3 shallow lakes obtained from a spectrophotometric study, *New Zealand J. of Marine and Freshwater Res.*, Vol. 17, pp. 445-459.
- Davies-Colley, R.J., and Vant, W.N. (1987) Absorption of light by yellow substance in freshwater lakes, *Limnol. Oceanogr.* Vol. 32, pp. 416-425.
- Dennis, J.E. Jr., and Schnabel, R. B. (1996) Numerical Methods for Unconstrained Optimization and Nonlinear Equations, *Classics in Applied Mathematics*, 16, SIAM, Philadelphia, 378 p.
- Effler, S.W., Perkins, M.G., and Wagner, B.A. (1991) Optics of Little Sodus Bay, *Great Lakes Res.*, Vol. 17,(1), pp. 109-119.
- Ferrari, G.M., and Tassan, S. (1991) On the accuracy of determining light absorption by "Yellow substance" through measurements of induced fluorescence, *Limnol. Oceanogr.*, Vol. 36, pp. 777-786.
- Gagosian, R.B., and Stuermer, D.H. (1977) The cycling of biogenic compounds and their diagenetically transformed products in seawater, *Marine Chemistry*, Vol. 5, pp. 605-611.
- Gallie, E.A. (1994) Optical calibration parameters for water-colour models from Swan lake, Northern Ontario, *Can. J. Remote Sensing*, Vol. 20, pp. 156-161.
- Gege, P. (1998) Lake Constance: Yellow substance measurements in 1998, *DLR International Report IB 552-9/99*, 17 p.
- Gege, P. (2000) Gaussian model for yellow substance absorption spectra, Proc. of the XV Conference of Ocean Optics, Monaco, 9 pp. (CD-ROM)
- Green, S.A., and Blough, N.V. (1994) Optical absorption and fluorescence properties of chromophoric dissolved organic matter in natural waters, *Limnol. Oceanogr.*, Vol. 39, pp. 1903-1916.
- Hoge, F.E., Vodacek, A., and Blough, N.V. (1993) Inherent optical properties of the ocean: Retrieval of the absorption coefficient of chromophoric dissolved organic matter from fluorescence measurements, *Limnol. Oceanogr.*, Vol. 38,(7), pp. 1394-1402.
- Højerslev, N. K. (1980) On the origin of yellow substance in the marine environment, *Oceanogr. Rep.*, Univ. Copenhagen, Inst. Phys. 42, 35 p.
- Højerslev, N.K., and Aas, E. (1998) Spectral light absorption by Gelbstoff in coastal waters displaying highly different concentrations, Proc. Ocean Optics XIV, Hawaii 1998, 8pp. (CD-ROM).
- Jerlov, N.G. (1968) *Optical Oceanography*, Elsevier, Amsterdam.
- Kalle, K. (1938) Zum Problem des Meereswasser farbe, *Ann. Hydrol. Mar. Mitt.*, Vol. 66, pp. 1-13.
- Kalle, K. (1966) The problem of gelbstoff in the sea, *Oceanogr.Mar.Biol.Annu.Rev.*, Vol. 4, pp. 91-104.
- Kallio, K. (1999) Absorption properties of dissolved organic matter in Finnish lakes, Proc.Estonian Acad. Sci. Biol. Ecol., Vol. 48,(1), pp. 75-83.
- Karlsson, S., Peterson, A., Håkansson, K., and Ledin, A. (1994) Fractionation of trace metals in surface water with screen filters, *The Sci. of the Total Env.*, Vol. 149, pp. 215-223.
- Kirk, J.T. (1976) Yellow substance (Gelbstoff) and its contribution to the attenuation of photosynthetically active radiation in some inland and coastal south-eastern Australian waters, *Aust.Mar.Freshwater Res.*, Vol. 27, pp. 61-71.
- Kirk, J.T.O. (1980) Spectral absorption properties of natural waters: Contribution of the soluble particulate fractions to light absorption in some inland waters of south-eastern Australia, *Aust.Mar.Freshwater Res.*, Vol. 31, pp.287-296.
- Kirk J.T.O., (1983) *Light and photosynthesis in aquatic ecosystems*, Cambridge Univ. Press, Cambridge, 401 p.

Optical Properties of Dissolved Organic Matter in Lakes

- Kopelevich, O.V. (1983) Factors determining the optical properties of the seawater, *Ocean Optics*, Nauka, Moscow, *J*, pp. 150-166.
- Kowalczuk, P., and Kaczmarek, S. (1996) Analysis of temporal and spatial variability of Yellow substance absorption in the southern Baltic, *Oceanologia*, Vol. 38, pp. 3-32.
- Kowalczuk, P. (1999) Seasonal variability of yellow substance absorption in the surface layer of the Baltic Sea, *J. Geophys. Res.*, Vol. 104, pp. 30,047-30,058.
- Ledin, A., Karlsson, S., Düker, A., and Allard, B. (1993) Applicability of Photon Correlation Spectroscopy for measurement of concentration and size distribution of colloids in natural waters, *Analytica Chimica Acta*, Vol. 281, pp. 421-428.
- Lundgren, B. (1976) Spectral transmittance measurements in the Baltic. Rep. Dept. Phys. Oceanogr., Univ. Copenhagen. 30, 38p.
- Miller, L.W., Johannessen, S., and Kuhn, P. (2000) The optical properties of dissolved organic matter (DOM) in coastal and open waters, Proc. of the XI Conference of Ocean Optics, Monaco 2000. 6pp. (CD-ROM).
- Mohr, M., and Sandström, A. (1996) Comparison between measurements and simulations with WASP and the MIUU model, Wind Energy Report WE 96:01. Dept. of Meteorology, Uppsala University, 1996, 48 p.
- Morel, A., and Prieur, L. (1977) Analysis of variations in ocean color, *Limnol. Oceanogr.*, Vol. 22, pp. 709-722.
- Mäekivi, S., and Arst, H. (1996) Estimation of the concentration of yellow substance in natural waters by beam attenuation coefficient spectra, Proc. Estonian Acad. Sci. Ecol. Vol. 6, (3/4), pp. 108-123.
- Nayfeh, A.H. (1981) *Introduction to perturbation techniques*, John Wiley & Sons, New York Chichester Brisbane Toronto.
- Nelson, J.R., and Guarda, S. (1995) Particulate and dissolved spectral absorption on the continental shelf of the southeastern United States., *J. Geophys. Res.*, Vol. 100, pp. 8715-8732.
- Nyquist, G. (1979) Investigations of some optical properties of seawater with special reference to lignin sulfonates and humic substances. Ph.D Thesis, Göteborgs Universitet, 200 p.
- Okami, N., Kishino, M., Sugihara, S., Takematsu, N., and Unoki, S. (1982) Analysis of ocean color spectra. 3. Measurements of optical properties of sea water, *J. Oceanogr. Soc. Jan*, Vol. 38 pp. 362-372.
- Strömbeck, N., and Pierson, D.C. (2001). The effects of variability in the inherent optical properties on estimations of chlorophyll *a* by remote sensing in Swedish freshwaters, *The Sci. of the Total Env.*, Vol. 268, pp. 123-137.
- Stuermer, D.H. (1975) The Characterization of Humic Substances in Sea Water, Ph.D Thesis, Mass. Inst. Technol. Woods Hole Oceanogr. Inst.
- Vodacek, A., Blough, N.V., DeGrandpre, M.D., Peltzer, E.T., and Nelson, R.K. (1997). Seasonal variations of CDOM and DOC in the Middle Atlantic Bight: Terrestrial inputs and photooxidation, *Limnol. Oceanogr.*, Vol. 42, pp. 674-686.
- Vähätalo, A.V., Salkinoja-Salonen, M., Taalas, P., and Salonen, K. (2000) Spectrum of the quantum yield for photochemical mineralization of dissolved organic carbon in a humic lake. *Limnol. Oceanogr.*, Vol. 45, pp. 664-676.
- EN1484, 1997. Water Analysis – Guidelines for the Determination of Total Organic Carbon (TOC) and Dissolved Organic Carbon (DOC). European Committee for Standardization.

Received: 4 July, 2001

Revised: 17 December, 2001

Accepted: 30 September, 2002

Addresses:

Liis Sipelgas,
Helgi Arst,
Ants Erm,
Tarmo Soomere,
Marine Systems Institute
At Tallinn Technical University,
Akademia tee 21B
12618 Tallinn, Estonia.

Email: liis@sea.ee
helarst@online.ee

Kari Kallio
Finnish Environmental Institute,
P.O.Box 140,
FIN-00251 Helsinki,
Finland.

Peeter Oja,
Inst. of Applied Mathematics,
University of Tartu,
J. Liivi 2,
50409 Tartu,
Estonia.